MINERAL RESOURCES
www.csiro.au

UNCOVER Cloncurry

Osborne Cu-Au deposit

Integrated Petrophysical and Geochemical Analyses

Michael Gazley, Benjamin Patterson, James Austin, John Walshe

EP165511

21st October 2016

Client: Geological Survey of Queensland; Chinova Resources Ltd

Queensland Government

Geological Survey of Queensland
Industry Priorities Initiative

chinova resources

CSIRO Mineral Resources

Citation

Gazley MF, Patterson BO, Austin JR, and Walshe JL (2016) Uncover Cloncurry – Osborne Cu-Au deposit: Integrated Petrophysical and Geochemical analyses. CSIRO, Australia, pp. 25.

Copyright

Important disclaimer

Contents

Acknowledgments iv

1 Introduction 1

2 Geological Setting 3

2.1 Host Rocks and Structural Setting 3

2.2 Metamorphism and Alteration 3

2.3 Geophysical Expression 4

3 Deposit Chemistry 6

3.1 Host rock geochemistry 6

3.2 Associated/anomalous elements 6

4 Deposit Mineralogy 7

4.1 XRF maps 7

4.2 SEM maps 7

4.3 Micro-CT 11

5 Deposit Petrophysics 12

5.1 Density, Magnetic Susceptibility and Remanence 12

5.2 Remanent Magnetisation 15

5.3 Alternating Field Demagnetisation (AFD) 17

6 Structural Controls 19

6.1 Structural Geology 19

6.2 AMS 19

7 Geophysics of the Deposit 22

8 Conclusion 23

9 References 24

Figures

Figure 1: Local geological map for the area surrounding the Osborne and Kulthor deposits. M= Mesozoic sandstone and siltstone, Pkr = mainly schist, meta-arenite, slate, phyllite; Cz = sand, silt, gravel: alluvial colluvial and residual. 4

Figure 2: Reduced to pole (RTP) magnetic image of the area surrounding the Osborne and Kulthor deposits. 5

Figure 3: Cu vs Au from the Chinova dataset for drill hole TTNQ0364 6

Figure 4: TIMA maps of unmineralised samples with mineral abbreviations after Whitney & Evans (2010). Field of view = 21 mm. 8

Figure 5: TIMA maps of mineralised samples with mineral abbreviations after Whitney & Evans (2010). Field of view = 21 mm 9

Figure 6: (a) Hematite/magnetite, total Ti phase, and amphibole abundance from TIMA data, and Au and Cu concentration from assay data plotted for drill hole TTNQ364; (b) as for a, but quartz, biotite, and total carbonate abundance. 10

Figure 7: (a) Total amphibole, chlorite, and Total Ti phase abundance from TIMA data, and Cu concentration (%) calculated from TIMA data plotted for drill hole OSH0067; (b) as for a, but quartz, biotite, and total carbonate abundance. 11

Figure 8: Plot of Magnetic Susceptibility (K) v Density (ρ). Data points coloured based on magnetic susceptibility values grading from blue (low susceptibility) to red (high susceptibility). 12

Figure 9: Plot of magnetite-hematite content versus magnetic susceptibility and density 13

Figure 10: Plot of density versus remanent magnetisation (J). The solid black circles are the NRM measurements and the hollow blue circles are the measurements made on the same samples after a liquid nitrogen bath. 14

Figure 11: Plot of Magnetic Susceptibility (K) v Koenigsberger ratio (Q). 15

Figure 12: Stereonet projection of the remanent magnetisation vectors from Osborne: black = NRM, blue = low temperature demagnetisation. Closed shapes plot in the lower hemisphere and open shapes plot in the upper hemisphere. Large open and closed shapes are the mean vectors for the upper and lower hemisphere orientations respectively. The open red triangles are the up-mast projections of the drill holes. 16

Figure 13: Stereonet projection of the NRM and low temperature demagnetisation vectors for the correctly oriented samples. Circles = NRM, squares = low temperature demagnetisation. Samples OSB001, -002, and -010 are from drillhole OSHQ0067 and OSB024 is from TTNQ0364. 17

Figure 14: Stereonet projection of AF demagnetisation measurements from selected Osborne samples. 18

Figure 15: AMS results for all Osborne samples. P is the degree of anisotropy and T is a measure of the oblateness of the ellipsoid; positive = oblate (foliation), negative = prolate (lineation) ... 19

Figure 16: AMS results for samples from drill holes OSHQ0067 (A) and TTNQ0364 (B). 20

Figure 17: 1st vertical derivative of the reduced to pole magnetic data over the Osborne-Kulthor area, indicates that the main north to north-northwest magnetic high is truncated by a number of northeast to east-northeast structures. 21

Tables

Table 1 Samples from Osborne and analyses performed as part of this project. 1

Acknowledgments

Uncover: CLONCURRY was funded in Round 3 of the Industry Priorities Initiative in 2015, for CSIRO to work with the Geological Survey of Queensland (GSQ) and industry partners (including MIM-Glencore, Exco-Copperchem, Minotaur, Altona, CST, Sandfire, Hammer Metals, and Chinova Resources) in developing mineral systems based exploration in the Mount Isa Eastern Succession. Additional funding comes from CSIRO Mineral Resources.

The authors are grateful to Chinova Resources for accommodation and logistical support during our field campaign, and for access to their data on the drill holes and Osborne area. Particular thanks are due to Damian Jungmann for his on-site assistance.

We acknowledge the reviews of Clive Foss and Alistair White on a draft of this report.

1 Introduction

This report, which is part of CSIRO's *Uncover: CLONCURRY* project, focusses on the geochemistry, mineralogy and petrophysics of the Osborne Cu-Au deposit.

Table 1 presents all the samples collected from Osborne as part of this study, and the nature of analyses conducted on them. Samples may not have been worked on for a variety of reasons, such as breaking during transport or during sample preparation.

For the entire catalogue of petrophysical and mineralogical data, readers are directed to the CSIRO Data Access Portal (DAP): http://doi.org/10.4225/08/5806a55f5797f (Patterson et al., 2016). Available data includes measurements and calculations of magnetic susceptibility, density, remanent magnetisation, and anisotropy of magnetic susceptibility as well as all scanning electron microscope mineralogy maps, X-ray fluorescence images and micro CT scans.

In depth explanations of the petrophysical, geophysical, mineralogical, and geochemical methods and terminology used in this report are available in 'Uncover Cloncurry – Background on Techniques and Methods' (Gazley et al., 2016).

Table 1 Samples from Osborne and analyses performed as part of this project.

Sample	Drillhole	From (m)	To (m)	TIMA	µXRF	µCT	Geo chem	Mag Sus	AMS	Density	Remanence
OSB001	OSHQ0067	42.60	42.75	Y	-	-	-	Y	Y	Y	Y
OSB002	OSHQ0067	58.00	58.15	Y	-	-	-	Y	Y	Y	Y
OSB003	OSHQ0067	61.20	61.35	Y	-	-	-	Y	Y	Y	Y
OSB004	OSHQ0067	67.30	67.40	-	-	-	-	-	-	-	-
OSB005	OSHQ0067	69.60	69.80	Y	-	-	-	Y	Y	Y	Y
OSB006	OSHQ0067	73.47	73.70	-	-	-	-	Y	Y	Y	Y
OSB007	OSHQ0067	73.95	74.10	Y	-	-	-	Y	Y	Y	Y
OSB008	OSHQ0067	76.76	76.90	-	-	-	-	-	-	-	-
OSB009	OSHQ0067	86.90	87.05	Y	-	-	-	Y	Y	Y	Y
OSB010	OSHQ0067	95.80	96.05	Y	-	-	-	Y	Y	Y	Y
OSB011	OSHQ0067	100.00	100.60	-	-	-	-	-	-	-	-
OSB012	OSHQ0067	101.90	102.30	-	-	-	-	-	-	-	-
OSB013	OSHQ0067	103.05	103.15	-	-	-	-	-	-	-	-
OSB014	OSHQ0067	109.65	109.80	Y	-	-	-	-	-	-	-
OSB015	OSHQ0067	111.30	111.45	Y	-	-	-	Y	Y	Y	Y
OSB016	OSHQ0067	115.15	115.35	-	-	-	-	-	-	-	-
OSB017	OSHQ0067	121.73	121.93	-	-	-	-	Y	Y	Y	Y
OSB018	TTNQ364	222.30	222.45	Y	-	-	-	Y	Y	Y	Y
OSB019	TTNQ364	246.35	246.55	-	-	-	-	-	-	-	-
OSB020	TTNQ364	258.60	258.80	-	-	-	-	-	-	-	-
OSB021	TTNQ364	265.25	265.40	Y	-	-	-	Y	Y	Y	Y
OSB022	TTNQ364	296.00	296.15	Y	-	-	-	Y	Y	Y	Y
OSB023	TTNQ364	297.00	297.30	Y	-	-	-	Y	Y	Y	Y
OSB024	TTNQ364	297.85	298.00	Y	-	-	-	Y	Y	Y	Y

OSB025	TTNQ364	326.20	326.40	Y	-	-	-	Y	Y	Y	Y
OSB026	TTNQ364	328.70	328.85	-	-	-	-	Y	Y	Y	Y
OSB027	TTNQ364	330.60	330.80	Y	-	-	-	Y	Y	Y	Y
OSB028	TTNQ364	332.75	332.94	Y	-	-	-	Y	Y	Y	Y
OSB029	TTNQ364	336.15	336.30	Y	-	-	-	Y	Y	Y	Y
OSB030	TTNQ364	337.20	337.35	Y	-	-	Y	Y	Y	Y	Y
OSB031	TTNQ364	344.55	344.70	Y	-	-	-	Y	Y	Y	Y
OSB032	TTNQ364	364.90	365.05	-	-	-	Y	Y	Y	Y	Y
OSB033	TTNQ364	372.30	372.45	-	-	-	Y	Y	Y	Y	Y
OSB034	TTNQ364	375.40	375.50	-	-	-	-	Y	Y	Y	Y
OSB035	TTNQ364	424.85	425.00	Y	-	-	-	Y	Y	Y	Y
OSB036	TTNQ364	431.15	431.30	Y	-	-	Y	Y	Y	Y	Y
OSB037	TTNQ364	450.35	450.55	Y	-	-	-	Y	Y	Y	Y
OSB038	TTNQ364	461.15	461.30	Y	-	-	-	Y	Y	Y	Y
OSB039	TTNQ364	467.50	467.70	Y	-	-	-	Y	Y	Y	Y
OSB040	TTNQ364	478.30	478.40	Y	-	-	-	Y	Y	Y	Y
OSB041	TTNQ364	481.20	481.35	-	-	-	-	Y	Y	Y	Y
OSB042	TTNQ364	489.95	490.15	Y	-	-	Y	Y	Y	Y	Y

2 Geological Setting

2.1 Host Rocks and Structural Setting

The Osborne Cu-Au deposit is located 130 km south of Cloncurry, with the ore bodies hosted within a predominantly metasedimentary sequence that is believed to be equivalent to the Soldiers Cap Group (Fisher, 2007). The main host rocks at Osborne are psammites with locally pelitic bands, banded ironstones, schist and associated migmatites (Adshead et al., 1998). The banded magnetite-quartz-apatite ironstones are continuous over 1.3 km along strike and are the significant host rock; they occur as two stratiform units that strike north-west and dip 25 – 60° to the north east. A gradational contact of several metres of interleaved magnetite-quartz and psammite are observed where the contacts of the ironstones and the host sequence are unaltered by mineralisation, whereas the upper contact of the lower ironstone is delineated by a strongly foliated anthophyllite schist (Adshead et al., 1998).

2.2 Metamorphism and Alteration

The metasedimentary rocks at Osborne have undergone partial melting, with U-Pb dating of titanite constraining the age of migmitisation, and thus peak metamorphism, to 1595 ± 5 Ma (Gauthier et al., 2001). This age is supported by monazite and metamorphic zircon ages from the Cannington Pb-Zn deposit at 1585 ± 5 Ma (Giles and Nutman, 2002, 2003). The Osborne area has been affected by albitisation events, which have been dated at ~1595 ± 5 Ma (Adshead, 1995; Perkins and Wyborn, 1998; Gauthier et al., 2001) and 1630 – 1650 Ma (Rubenach et al., 2008).

The age and source of the fluids that formed the Osborne deposit have been the subject of debate (Davidson et al., 1989; Adshead et al., 1998; Gauthier et al., 2001; Rubenach et al., 2001; Fisher, 2007; Fisher & Kendrick, 2008). Early studies concluded that the ore bodies were syngenetic exhalative deposits (Davidson et al., 1989; Davidson, 1992). However, as more drilling was conducted it was recognised that high-grade mineralisation is hosted by extensive coarse-grained hydrothermal quartz, termed ‘silica flooding’ (Adshead et al., 1998). Other workers have preferred an epigenetic model for the formation of the deposit, but have debated its age. $^{40}Ar/^{39}Ar$ ages from actinolite, hornblende and biotite in a metamorphic assemblage gives ages of 1595 ± 2 Ma and 1568 ± 3 Ma (Adshead et al., 1998), while metasomatic hornblende and biotite associated with mineralisation give ages of 1538 ± 2 Ma (Perkins & Wyborn, 1998). While Gauthier et al. (2001) used Re-Os systematics of two molybdenite samples that were associated with mineralisation to suggest that the deposit formed between 1600 and 1595 ± 5 Ma.

Fluid mixing is preferred as an ore-formation mechanism, with the mingling of oxidised and reduced fluids causing the precipitation of ore minerals, and the sulphur transported in the reduced fluid (Fisher, 2007). Modelling suggests that dominance of the reduced fluid phase is required to reach significant deposition of chalcopyrite associated with a redox switch. However, if the solid and fluid phases become too reduced, galena and sphalerite become over-saturated. The absence of galena and sphalerite from the ore assemblage, despite the presence of Pb and Zn at 100s to 1000s ppm in

the ore fluids suggests that the redox conditions at Osborne remained fixed within a narrow range throughout ore formation, probably as the result of rock-buffering.

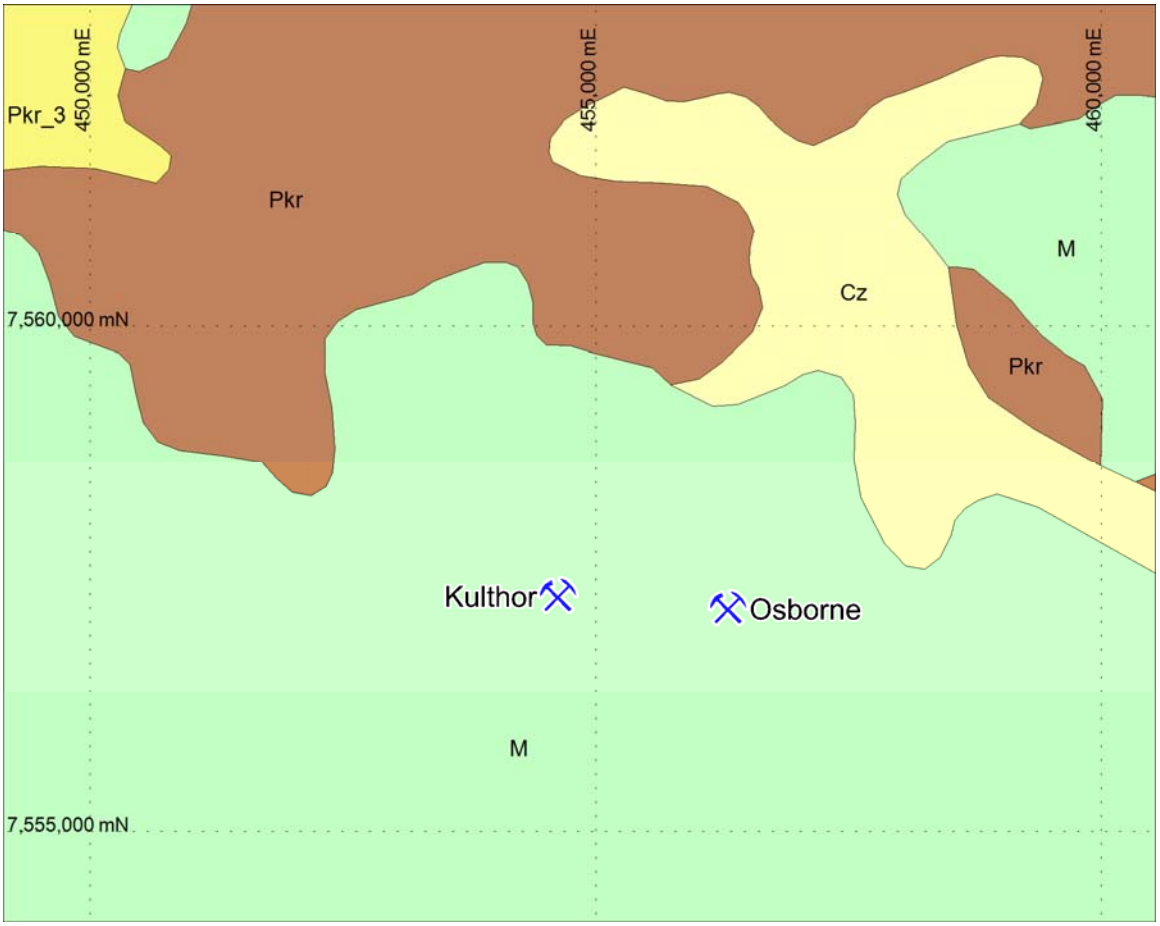

Figure 1: Local geological map for the area surrounding the Osborne and Kulthor deposits. M= Mesozoic sandstone and siltstone, Pkr = mainly schist, meta-arenite, slate, phyllite; Cz = sand, silt, gravel: alluvial colluvial and residual.

2.3 Geophysical Expression

The Osborne deposit sits on a prominent positive magnetic anomaly (Figure 2). As detailed later in this report, the extremely high magnetic susceptibility of the magnetite ironstone host rocks produces a significant self-demagnetisation effect that must be accounted for when modelling the deposit (Clark, 1988). Additionally, remanent magnetisation is typically easily overprinted in coarse grained magnetite and does not play a large role in perturbing the magnetic anomaly at Osborne. Early interpretations of the magnetic anomaly at Osborne yielded incorrect dip estimates for the ore body and two subsequent drill holes based off these interpretations did not intersect fresh copper mineralisation (Gidley, 1988). Once self-demagnetisation was properly integrated into the magnetic modelling, subsequent drillholes successfully intersected fresh copper mineralisation. The Osborne ore body produces both IP (Induced Polarisation) and EM (Electromagnetic) anomalies that are all broadly coincident. Time-domain EM results over the area produced decay constants between 2.9 and 3.5 ms indicating a strong conductor similar to results obtained over the Starra ore bodies (Gidley, 1988).

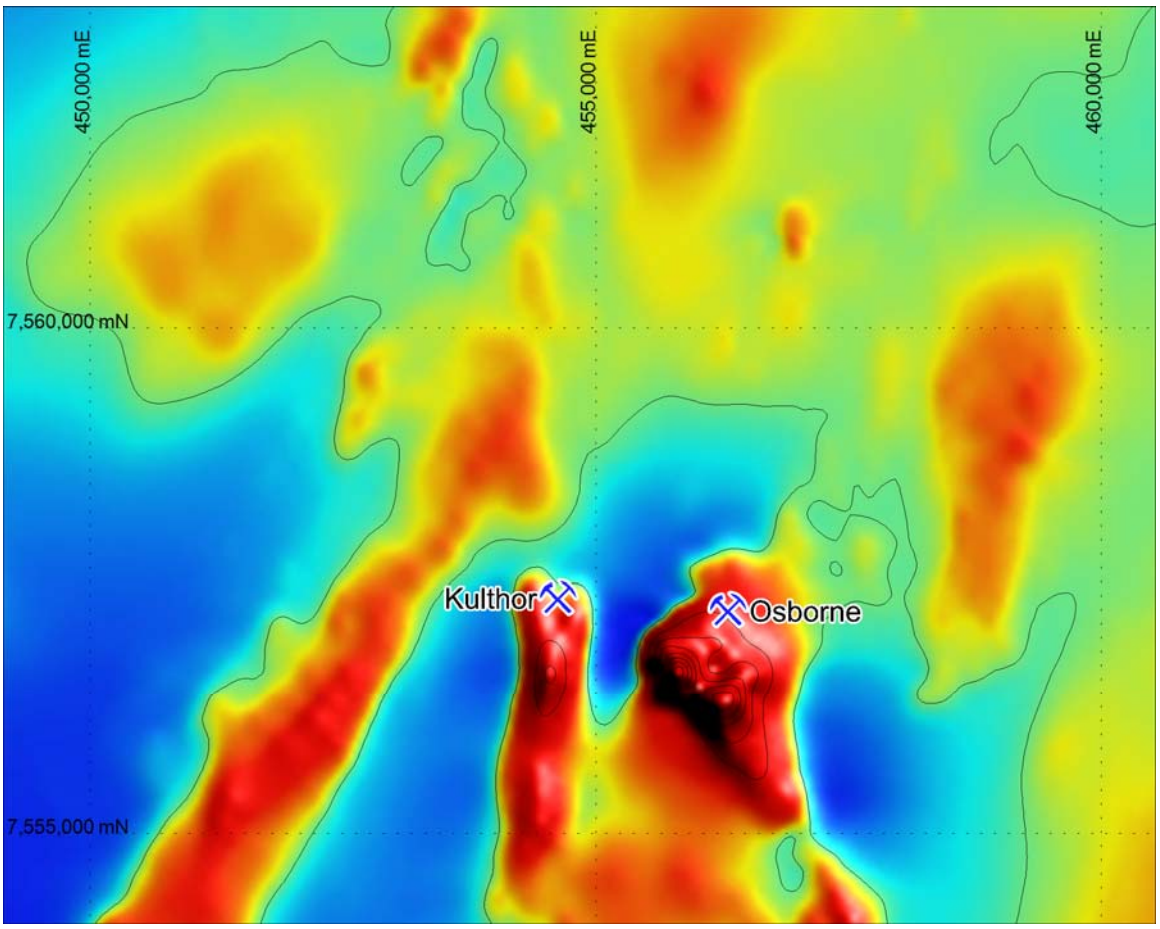

Figure 2: Reduced to pole (RTP) magnetic image of the area surrounding the Osborne and Kulthor deposits.

3 Deposit Chemistry

3.1 Host rock geochemistry

The only geochemsitry available for drill hole TTNQ0364 is for Cu and Au, and values are not continuous down the drill hole, with only selected samples taken for assay. OSHQ067 was a geotechnical drill hole that was sampled as it provided samples of the ironstones near the surface, but this drill hole was not assayed. This dataset does not allow for examination of geochemistry at Osborne.

3.2 Associated/anomalous elements

A plot of Cu vs Au shows a near-linear positive correlation for samples from drill hole TTNQ0364 (Figure 3).

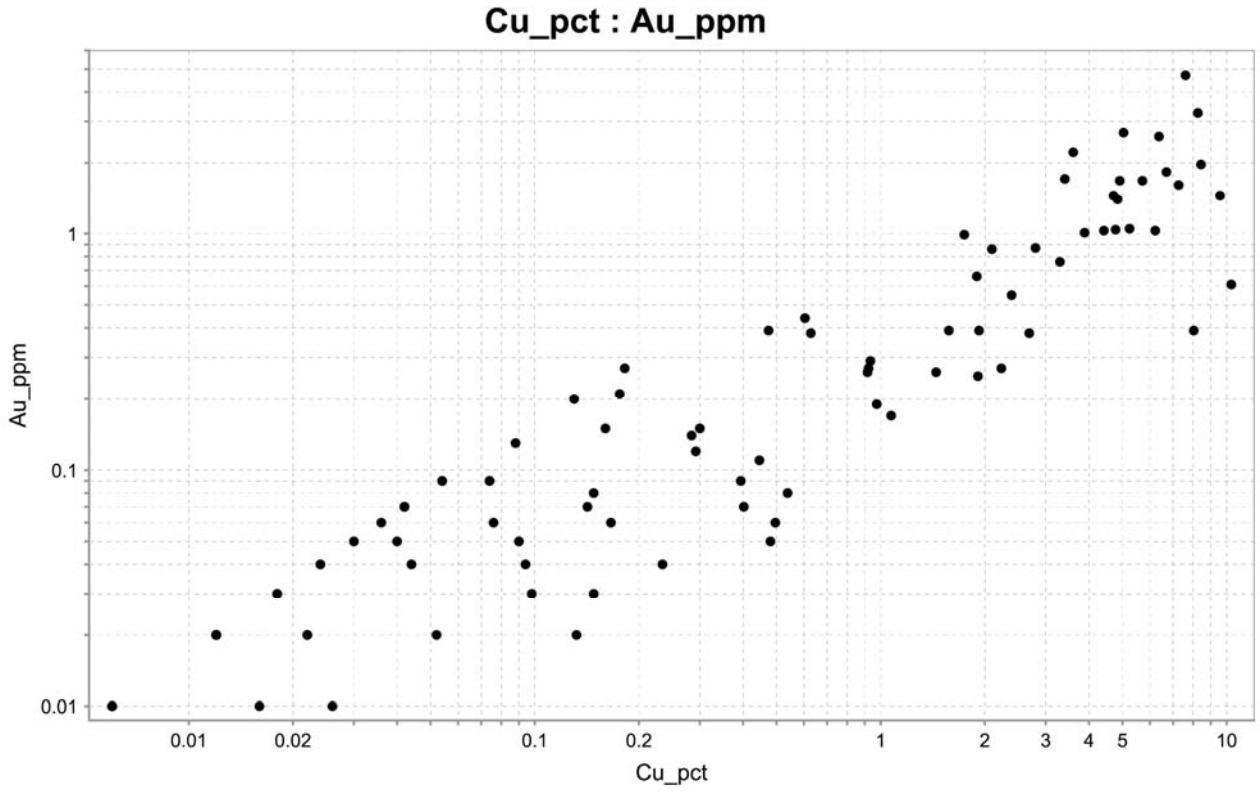

Figure 3: Cu vs Au from the Chinova dataset for drill hole TTNQ0364.

4 Deposit Mineralogy

4.1 XRF maps

No samples from Osborne were examined using µXRF (micro X-ray fluorescence).

4.2 SEM maps

Figure 4 presents TIMA (Tescan Integrated Mineral Analyser) maps of unmineralised samples from Osborne. OSB001 is a weathered banded-iron-formation (BIF) dominated by quartz and hematite with minor talc. OSB009 is a foliated schist with talc defining the fabric with minor biotite, rutile is the stable Ti-bearing phase. Sample OSB018 is logged as a retextured BIF with massive magnetite, which is a lot coarser than that in other BIF samples from Osborne. It contains abundant talc, with lesser biotite and chlorite on the margins of the recrystallised magnetite. Pyrite, quartz and apatite are present in lesser amounts. OSB025 and OSB031 are psammites with minor pyrite apparent in hand sample; they are dominated by quartz and albite with minor magnetite, apatite and biotite. Sample OSB025 may have minor disseminated garnets (indexed as chlorite in the TIMA data). Sample OSB037 is an albite-plagioclase-biotite-gedrite rock that is located in the footwall of mineralisation – this may be the upper contact to the lower ironstone, which is delineated by an anthophyllite schist. It is unclear whether the TIMA database is capable of differentiating between gedrite $(Mg,Fe)_5Al_2(Al_2Si_6)O_{22}(OH)_2$) and anthophyllite ($(Mg,Fe)_7Si_8O_{22}(OH)_2$) as amphiboles are notoriously difficult to classify reliably with the TIMA system. Also, it should be noted that at the peak metamorphic conditions that affected these rocks, the stable feldspar was likely plagioclase rather than albite, so if albite is present in this rock, it represents metasomatism/alteration and not the stable metamorphic assemblage.

Figure 5 presents TIMA maps for mineralised samples from Osborne. OSB007 is a BIF with 2.45 vol.% chalcopyrite which overprints a matrix dominated by magnetite and quartz. The chalcopyrite is intimately associated with chlorite and biotite, while in some places it is intergrown with apatite. OSB022 contains abundant pyrite overgrowths in a magnetite-BIF with minor quartz, talc and chlorite; chalcopyrite is a minor phase in this sample intergrown with pyrite. Sample OSB032 contains abundant chalcopyrite (33.8 vol.%) which overgrows well-formed subhedral magnetite, pyrite and quartz. Chlorite and apatite are present. In contrast to OSB032, sample OSB33 contains very little magnetite, and the matrix is dominated by quartz with pyrite overgrowing the chalcopyrite. OSB034 represents a coarse magnetite-pyrite rock with negligible chalcopyrite, minor apatite, and as for OSB032 and OSB33 no carbonate. Sample OSB036 is a mineralised biotite schist sample with quartz, minor albite and abundant biotite (which defines the foliation); chalcopyrite is included in the fabric. Minor dolomite is present and pyrite is intergrown with the biotite.

Down hole mineralogy for drill holes TTNQ364 (Fig 6) and OSH0067 (Fig 7) do not provide many insights into mineralogical zonation within the Osborne mineral system; except for the possibility of a minor carbonate halo around the mineralised zone (Fig 6b; 7b).

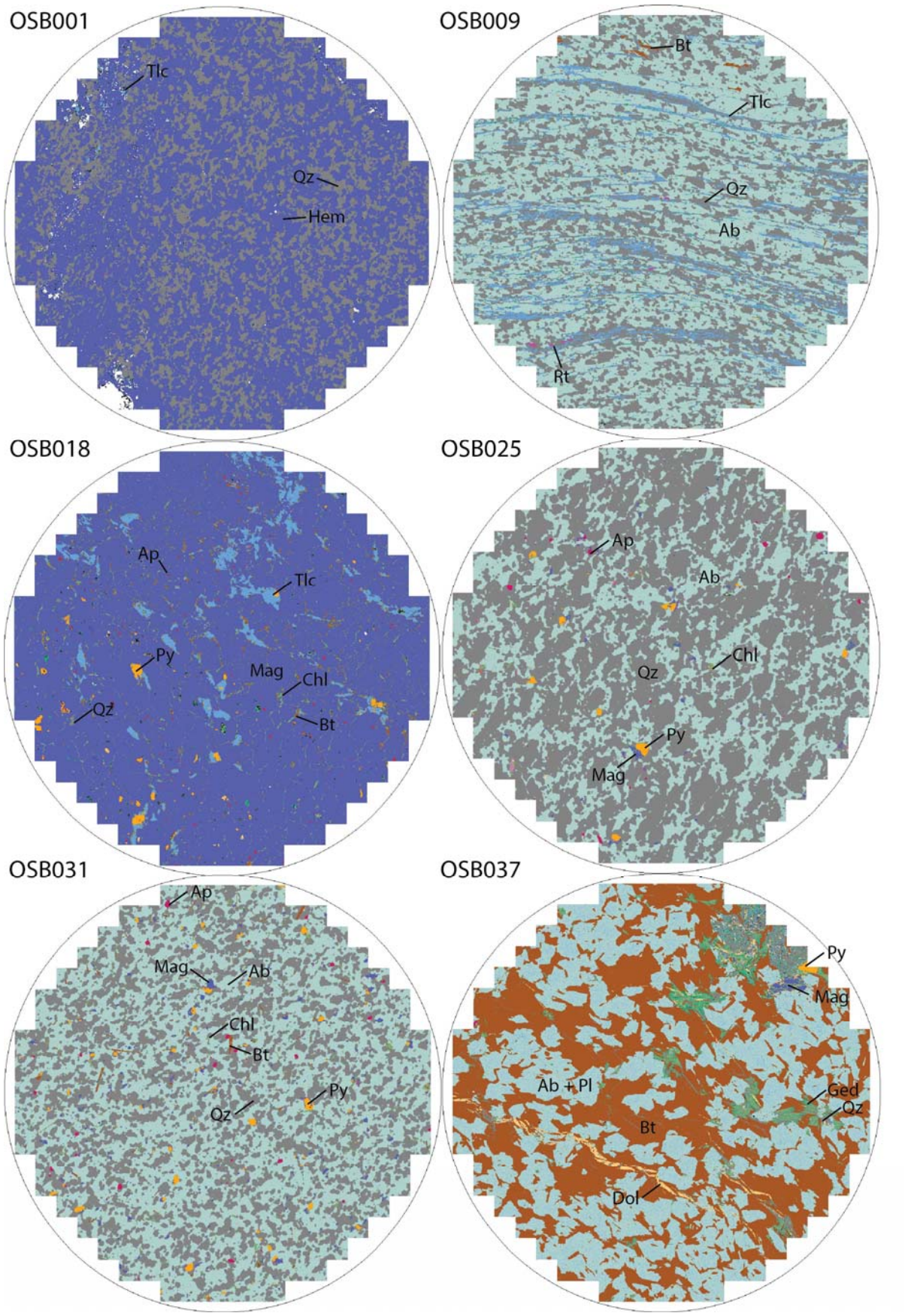

Figure 4: TIMA maps of unmineralised samples with mineral abbreviations after Whitney & Evans (2010). Field of view = 21 mm.

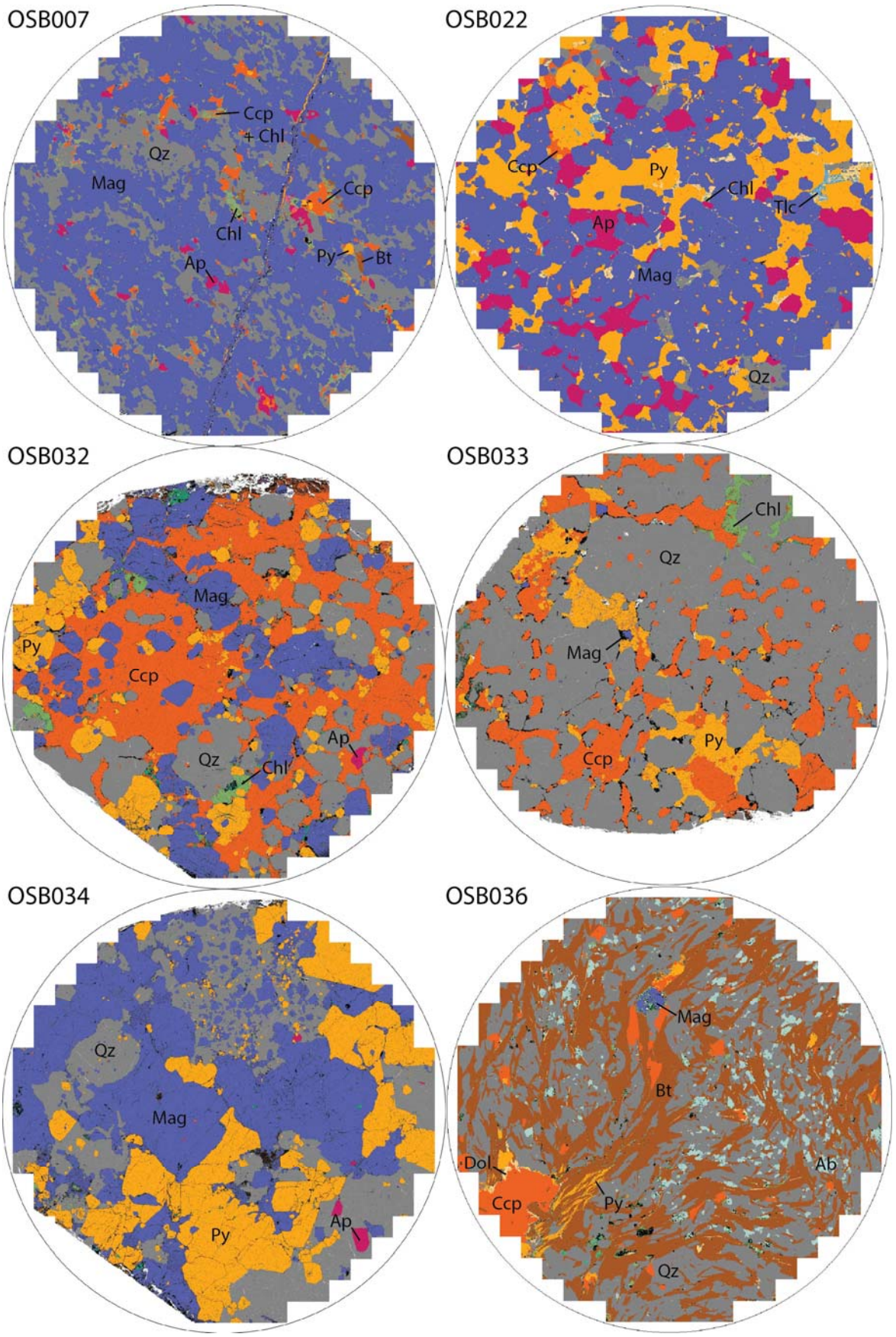

Figure 5: TIMA maps of mineralised samples with mineral abbreviations after Whitney & Evans (2010). Field of view = 21 mm.

Figure 6: (a) Hematite/magnetite, total Ti phase, and amphibole abundance from TIMA data, and Au and Cu concentration from assay data plotted for drill hole TTNQ364; (b) as for a, but quartz, biotite, and total carbonate abundance.

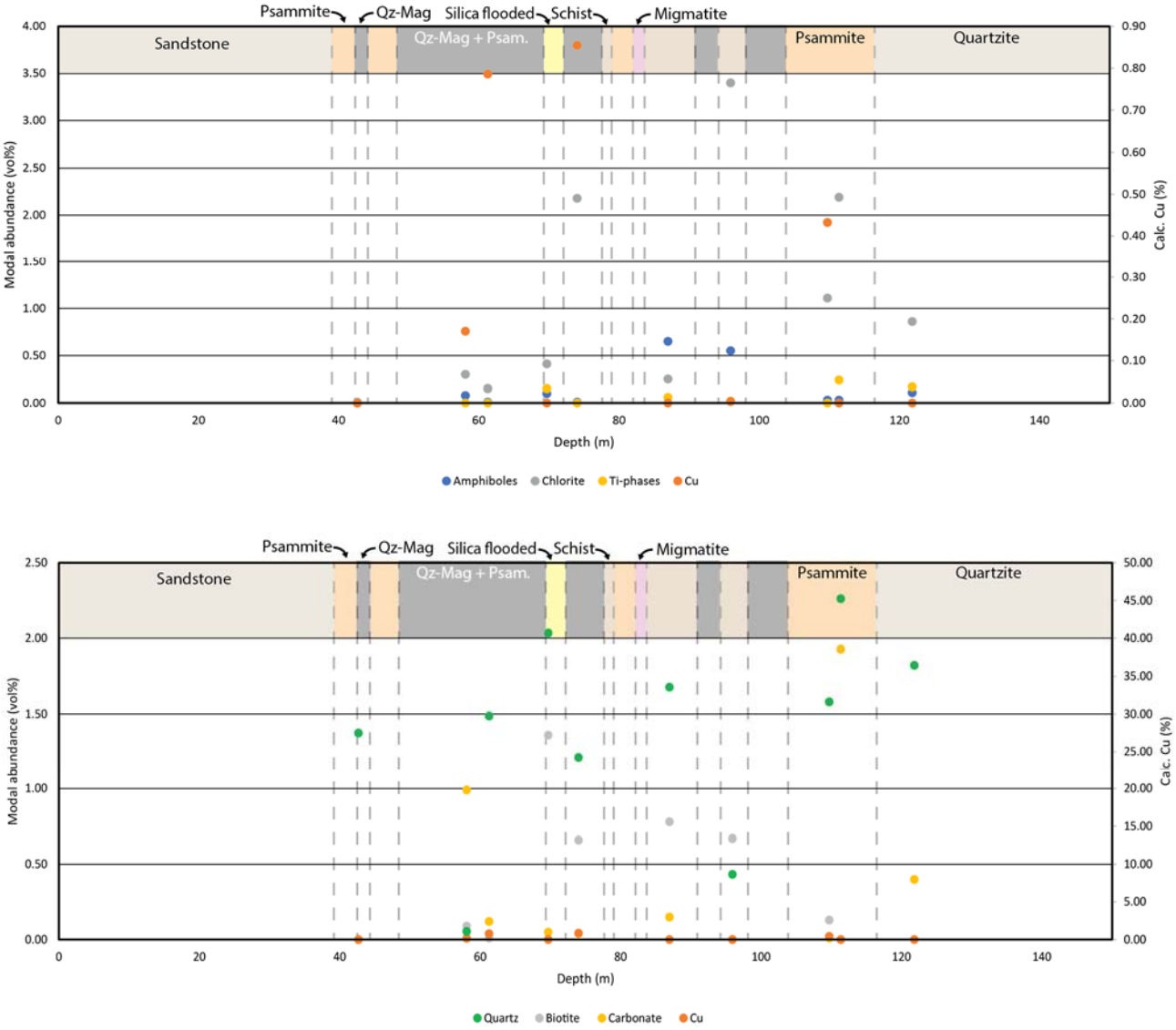

Figure 7: (a) Total amphibole, chlorite, and Total Ti phase abundance from TIMA data, and Cu concentration (%) calculated from TIMA data plotted for drill hole OSH0067; (b) as for a, but quartz, biotite, and total carbonate abundance.

Fisher (2007) argued that the reaction of quartz-magnetite banded ironstones with ore fluids resulted in the destruction of magnetite and the deposition of sulphides. The textures that we observe in the TIMA data here are largely consistent with that interpretation; some samples have almost no magnetite and abundant chalcopyrite (e.g. OSB033; Fig 5), but others show textures that may suggest stability of chalcopyrite and magnetite as the magnetites are largely subhedral (e.g. OSB032; Fig 5).

4.3 Micro-CT

No samples from Osborne were examined using µCT (micro computed tomography).

5 Deposit Petrophysics

5.1 Density, Magnetic Susceptibility and Remanence

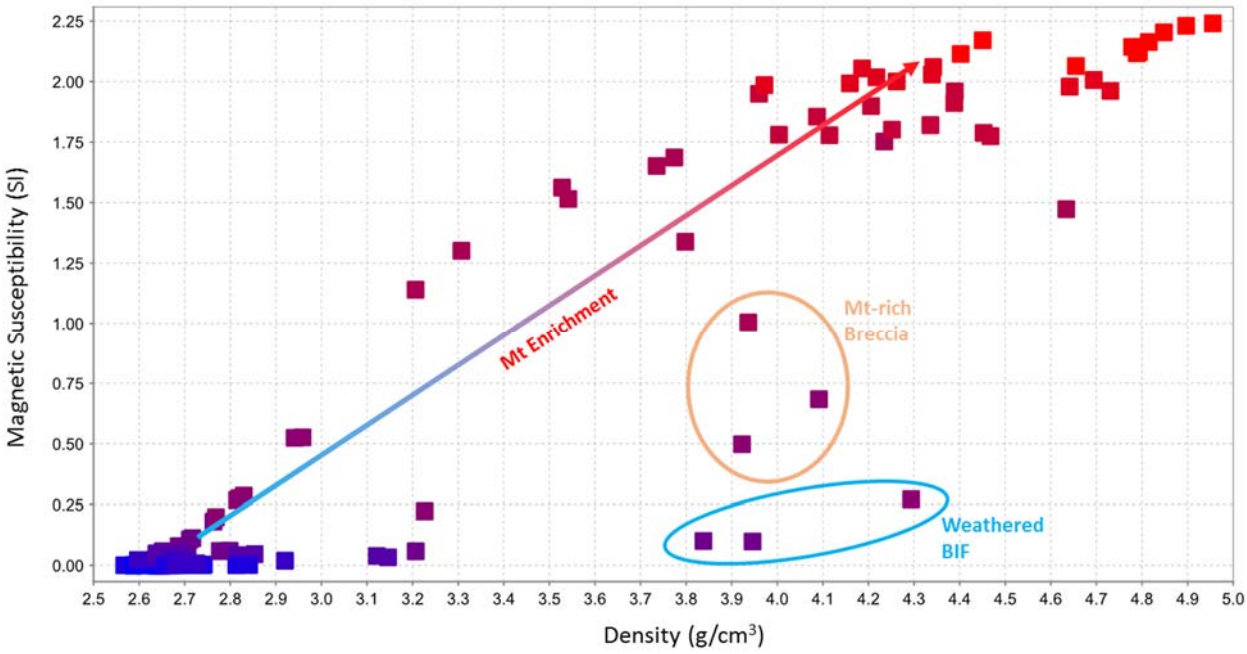

Figure 8: Plot of Magnetic Susceptibility (K) v Density (ρ). Data points coloured based on magnetic susceptibility values grading from blue (low susceptibility) to red (high susceptibility).

Figure 8 shows the plot of magnetic susceptibility (K) versus density (ρ). As is evident in the data, a large number of samples have extremely high K values, which are attributed to the extremely high magnetite content at Osborne. The most prominent trend is that of the magnetite enrichment – the linear increase of both density and magnetic susceptibility as magnetite content increases. A weathered hematite BIF sample plots at the bottom of the graph due to the high density and low susceptibility of hematite. A variably magnetite-rich mineralised breccia sits between the hematite BIF and the main magnetite trend. A high density of the sulphides shifts points to the right and away from the magnetite enrichment trend line.

The hematite BIF to magnetite enrichment trend is illustrated in Figure 9 with a graph of Magnetite-Hematite content (as determined by TIMA imagery) versus density and magnetic susceptibility. It should be noted that the TIMA cannot distinguish between magnetite and hematite, and subsequently groups the two together. Despite the grouping of magnetite with hematite, the overall trend is still valid. Samples with low ρ, low K and low magnetite-hematite content plot in the lower left sector of the graph. The variation of ρ and K with respect to magnetite-hematite correlates quite well, other than with the exception of a few samples within the range ~20 – 50 vol.% magnetite-hematite. TIMA imaging was carried out on only 1 sub-sample (of three) for each bulk sample whereas the density and magnetic susceptibility values used in Figure 9 are an average of all three sub-samples. In a case where the core sample is heterogeneous (e.g., it passes through a quartz/carbonate vein), the three sub samples may show vastly different petrophysical responses.

This is likely the case for the two samples that show a significantly lower density compared with their magnetic susceptibility as well as at least some of the others that show significant offsets from the trend. However, the sample with a high ρ and low K at 66 vol.% magnetite-hematite is simply an oxidised hematite BIF. Disregarding these three samples, the correlation between ρ and K and magnetite-hematite content is, as expected, quite strong.

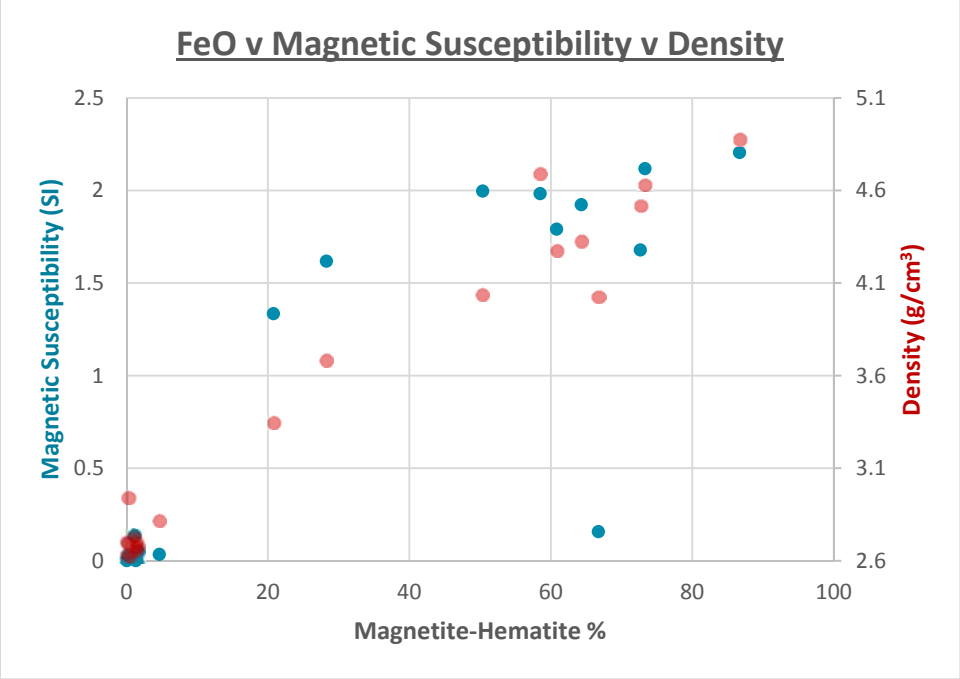

Figure 9: Plot of magnetite-hematite content versus magnetic susceptibility and density.

The plot of density versus remanent magnetisation is shown in Figure 10. Natural remanent magnetisation (NRM) increases with increasing density – similar to the trend of magnetic susceptibility. This suggests that the remanent magnetisation may be carried in the same highly susceptible magnetic mineral. A number of factors contribute to the non-linear spread of the data. Coarse-grained magnetite is more susceptible to having its NRM magnitude artificially enhanced by drilling induced magnetisation. It is not uncommon for rocks containing coarse grained magnetite to have remanent magnetization intensities enhanced by three or four times when compared to their original intensity (see Section 2.7 in Gazley et al., 2016). Finer grained magnetite generally retains a stable magnetisation for longer. Also, although hematite has a very low magnetic susceptibility, it can contribute significantly to remanent magnetisation.

The magnetisation of coarse grained magnetite, however, is usually quite soft and can often be substantially reduced by bathing the sample in liquid nitrogen as described by Schmidt (1993). The results of the low-temperature demagnetisation are also plotted on Figure 10. It is clear that the magnetite rich samples with high NRM values lost significant proportions (up to ~80%) of their magnetisation. The average soft component of magnetisation across all of the samples was 73%

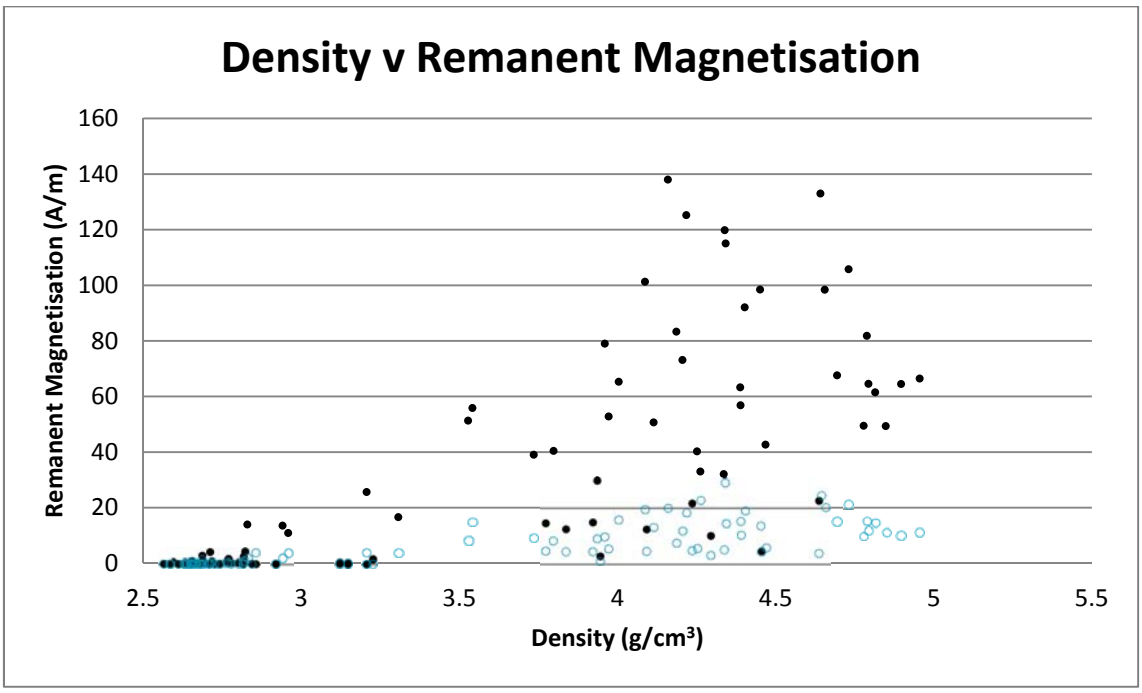

Figure 10: Plot of density versus remanent magnetisation (J). The solid black circles are the NRM measurements and the hollow blue circles are the measurements made on the same samples after a liquid nitrogen bath.

The plot of magnetic susceptibility (K) versus the Koenigsberger ratio (Q) is displayed in Figure 11. Two distinct groups are visible: variably mineralised, magnetite rich rocks and weakly magnetic hots rocks. As expected, the magnetite rich samples with their high susceptibilities have relatively low Q ratios – generally <1.8. The high Q ratio samples belong to the group of weakly magnetic hot rocks and the elevated Q values are of little significance as remanent magnetisation intensities for these samples are often less than 1 mA/m. The highest Q values were obtained from albite altered psammite. Ninety percent of the NRM magnitude was removed with low temperature demagnetisation, which significantly lowers the Q value to <1.

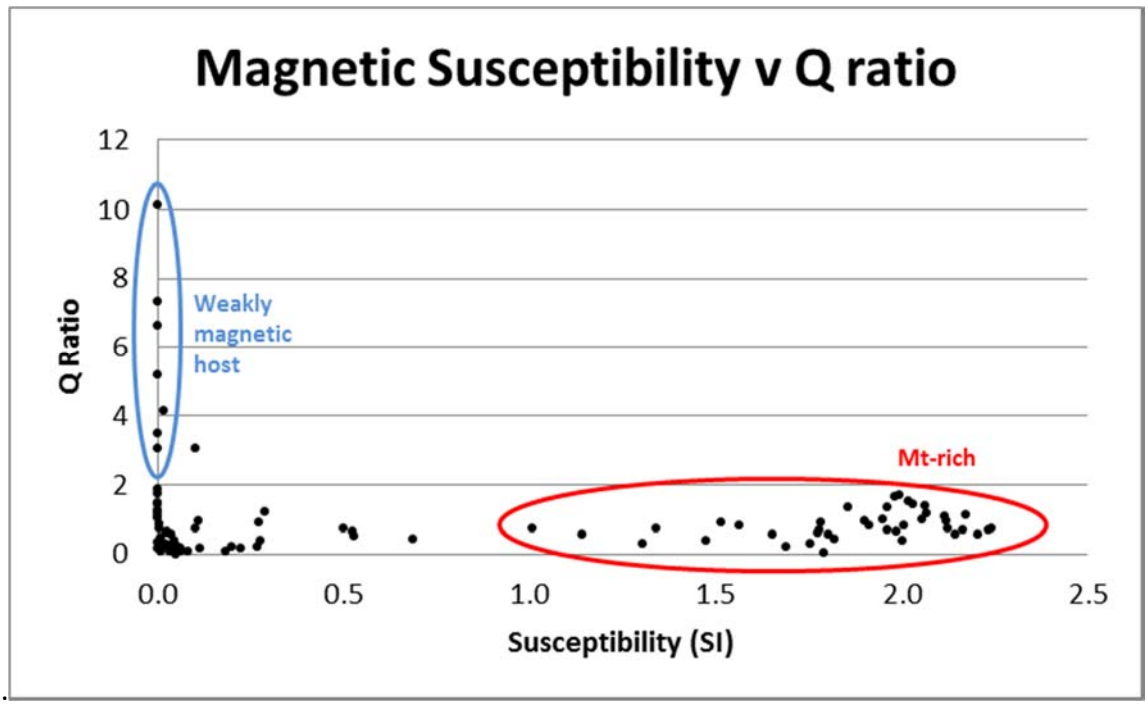

Figure 11: Plot of Magnetic Susceptibility (K) v Koenigsberger ratio (Q).

5.2 Remanent Magnetisation

Only 4 of the samples for this study had orientation information marked on the core. This meant that the only correctly oriented remanence directions came from a spread of samples far too small to be considered statistically robust. However, measurements were made on all specimens in order to measure their magnetisation intensities as discussed in Section 5.1. After measurement of all NRM values, the samples were 'cleaned' of their soft magnetisation using liquid nitrogen followed by alternating field (AF) demagnetisation (Section 5.3).

Work completed by Clark (1988) suggested that self-demagnetisation dominated over remanent magnetisation with regard to perturbing the anomaly of the Osborne ore body and associated ironstone units. This is due mainly to the fact that coarse grained magnetite is so prevalent at Osborne. Typically, magnetite grains larger than 1 – 10 µm contain more than one magnetic domain and are termed multi-domain (MD). These grains can be remagnetised simply by moving an internal domain wall, which requires little energy and can occur at low temperatures - so MD materials rarely retain stable remanent magnetisations.

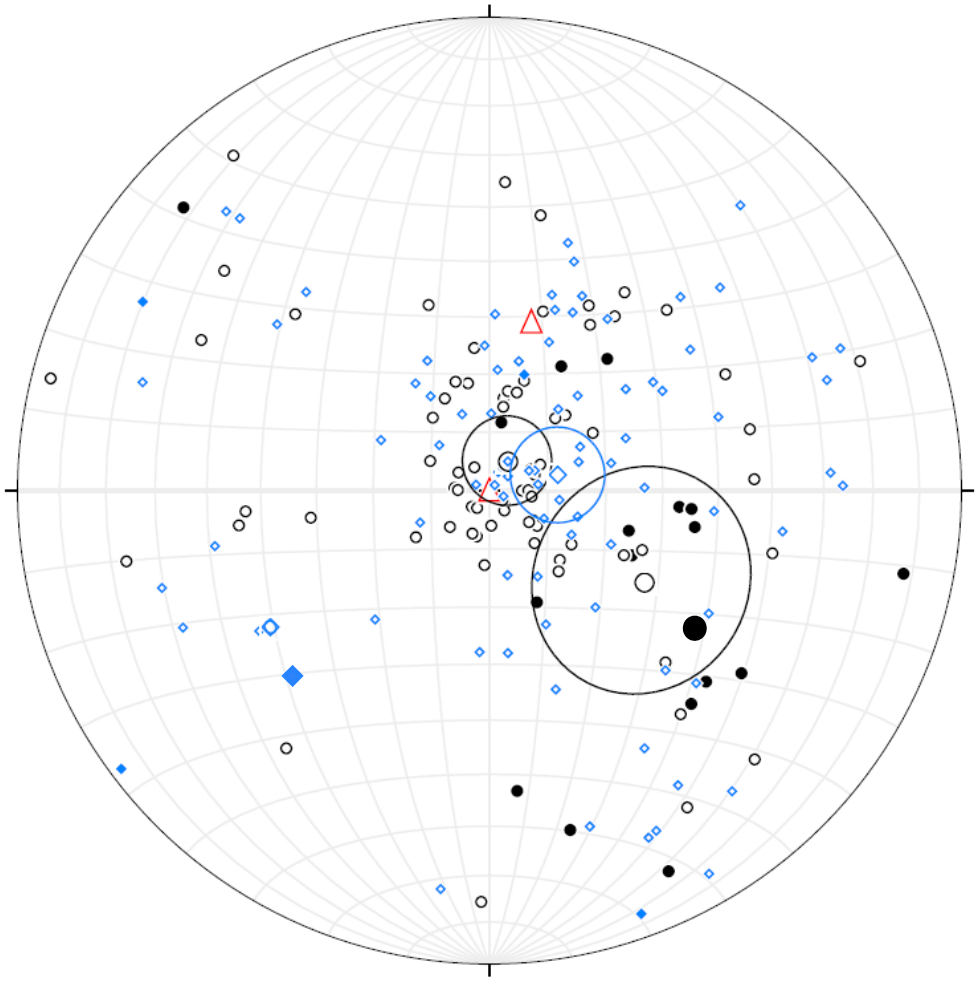

Figure 12: Stereonet projection of the remanent magnetisation vectors from Osborne: black = NRM, blue = low temperature demagnetisation. Closed shapes plot in the lower hemisphere and open shapes plot in the upper hemisphere. Large open and closed shapes are the mean vectors for the upper and lower hemisphere orientations respectively. The open red triangles are the up-mast projections of the drill holes.

The NRM measurements made by Clark correlate reasonably well with those measured in this study (Figure 12) and have a mean vector oriented sub-vertical upwards (+85°→030°). It should be noted however that the drill hole from which the majority of the samples were taken (TTNQ0364) lies within the bounds of the error margin of the mean vector (Figure 12), suggesting that these directions may be related – for instance that the remanent magnetization may be predominantly drilling induced.

As seen in Figure 12, the overall spread of the low temperature demagnetisation data remained very similar to that of the NRM values. Some differences to note include the shift of the mean upper hemisphere vector towards the east, further away from (but still proximal to) the drilling orientations, and the decrease in the number of data points in the lower hemisphere – reduced from 17 to 4.

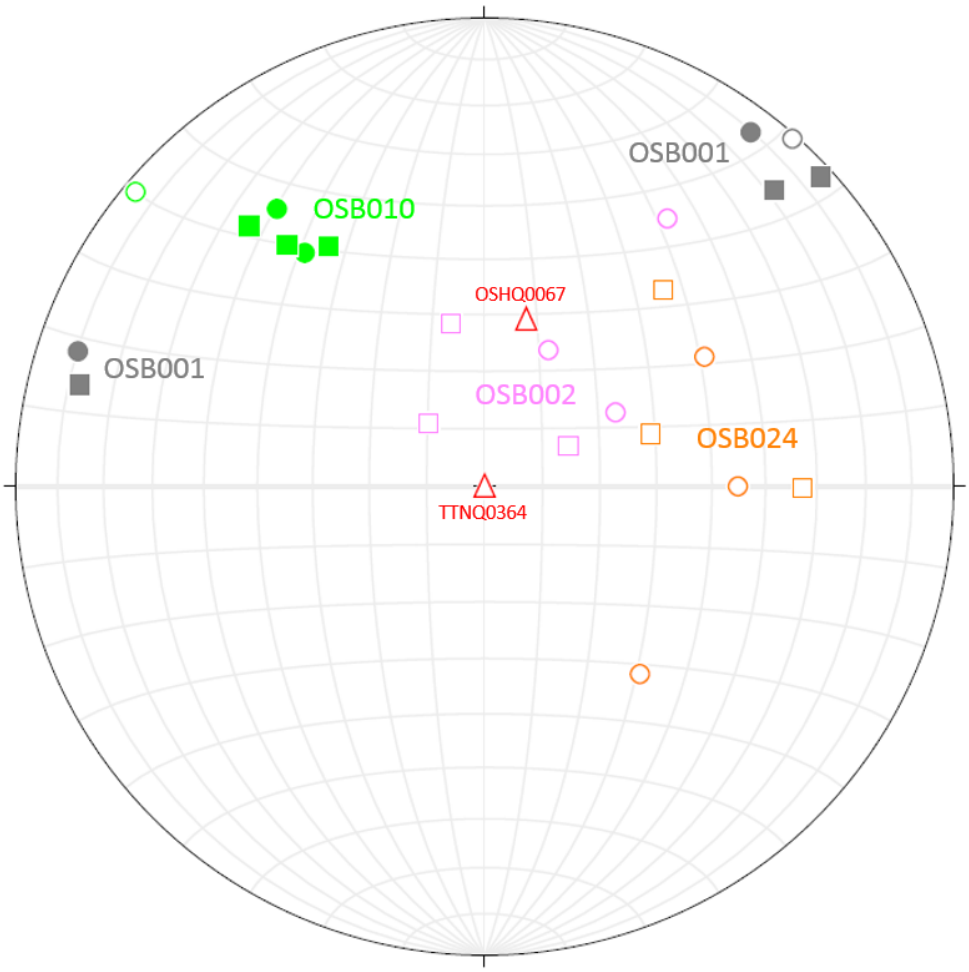

Figure 13: Stereonet projection of the NRM and low temperature demagnetisation vectors for the correctly oriented samples. Circles = NRM, squares = low temperature demagnetisation. Samples OSB001, -002, and -010 are from drillhole OSHQ0067 and OSB024 is from TTNQ0364.

Figure 13 shows the NRM and post low-temperature demagnetisation vectors for the samples that are known to have reliable orientations. OSB002 is a coarse grained magnetite ironstone and plots reasonably close to the drilling projection. This result is expected for coarse grain multi-domain (MD) magnetite that is easily overprinted or reset by drilling (Section 2.7 in Gazley et al., 2016).

5.3 Alternating Field Demagnetisation (AFD)

Alternating field demagnetisation (AFD) was initially carried out only on the correctly oriented samples, but later included other representative samples from both drill holes. Although the measured vectors are unreliable as the samples were not correctly oriented, the magnetisation intensity data are still useful for examination of the coercivity of the rock. Samples were subjected to peak fields of 140 mT (milli-Tesla) although many samples were completely demagnetised in fields far lower. In most cases, the remanent signal was overwhelmed by noise prior to reaching fields of 50 mT. This is especially true for samples with very little magnetisation intensity to begin with i.e. less than a few hundred A/m prior to AFD.

Of the four correctly oriented samples, three had well defined paths on the stereonet (Figure 14). Sample OSB001 (hematite-magnetite BIF) tracked from a sub-horizontal NE direction to a moderately plunging SE orientation. Principal component analysis of this sample indicates that the magnetisation may not be fully resolved. OSB010A has a stable westward demagnetisation path, although it is lost in noise after 60 mT indicating the sample has been fully demagnetised. Similarly, OSB002A tracks from the LN2 orientation (+75°→318°) westward and with decreasing upward plunge towards +10°→291° at 60 mT.

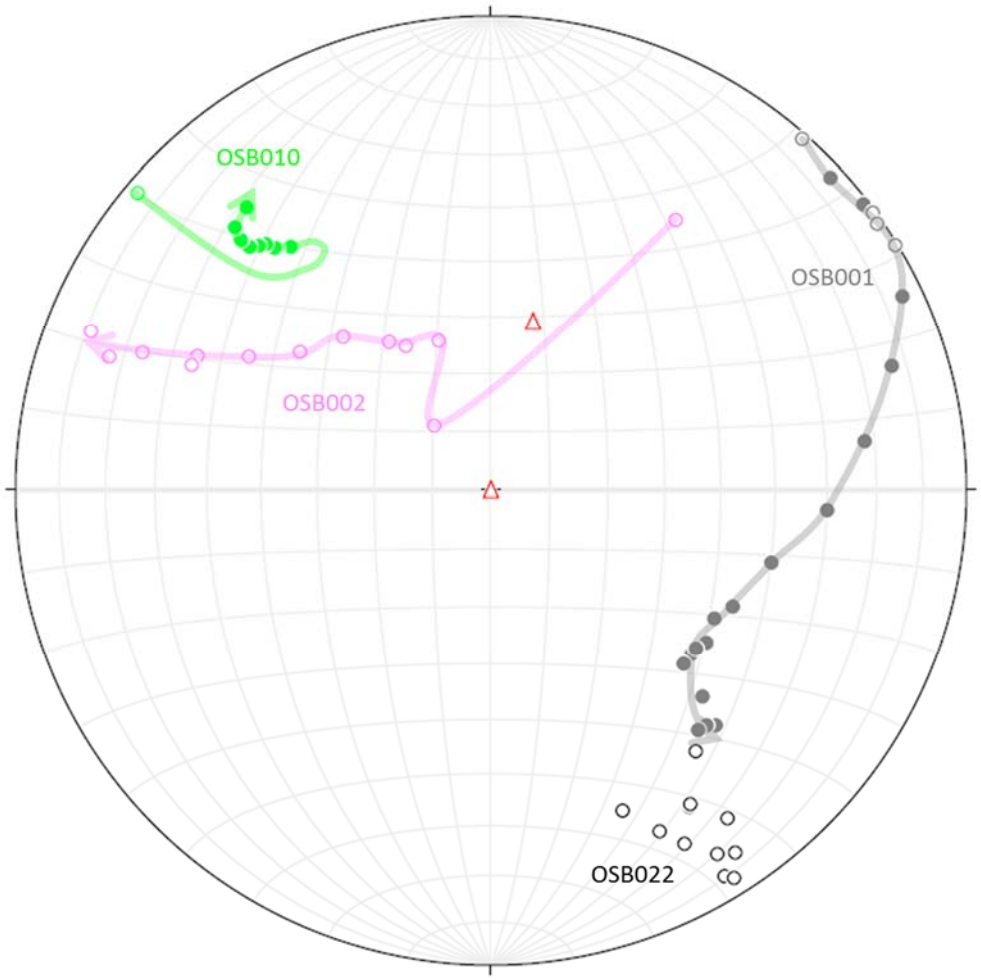

Figure 14: Stereonet projection of AF demagnetisation measurements from selected Osborne samples.

Despite being separated by only 15 m in the hole, samples OSB001 and OSB002 have very different magnetisations. Furthermore, none of the correctly oriented samples have magnetisation histories that appear to correlate. A number of the un-oriented samples appeared to show some correlation (e.g. OSB022 appears as the reflection of OSB010) but any use of this data to calculate a remanence direction at Osborne would be spurious. It is suggested that in order to fully understand the remanent magnetisation at Osborne, a larger suite of correctly oriented samples is needed. Although the correctly oriented samples appear to display ancient magnetisations, none of the samples resolved the same orientation, thus a dominant remanent magnetisation direction cannot be calculated from the data collected in this study.

6 Structural Controls

6.1 Structural Geology

The Osborne deposit is hosted in north to northwest trending ironstone units that dip moderately towards the northeast beneath 30-50 m of Mesozoic shale and sedimentary cover. Osborne lies in a lateral equivalent to the Mt. Norna quartzite in the Soldiers Cap Group. The ironstone units occur as laterally continuous bodies that are oriented sub-parallel to the northwest trending local S_2 fabric and shear zones (Duncan et al., 2014; Adshead et al., 1998).

6.2 AMS

The anisotropy of magnetic susceptibility (AMS) was measured for all of the Osborne samples to identify any strain-related magnetic fabrics. The results shown in Figure 15, have a large spread and no clear trends – partly due to the fact the samples are from two drill holes, but mainly due to the lack of correct sample orientations. There is a fairly even spread of data between foliation (oblate) and lineation (prolate) dominated samples (plot of T v P, Figure 15). The three axes which make up the AMS ellipsoid are K1 (long axis), K2 (intermediate axis), and K3 (short axis). The value of P in the following figures is the ratio of K1 to K3 and is a measure of the anisotropy. A P value of 1 means the sample is isotropic and any value increasing above 1 corresponds to increasing anisotropy. The resultant vectors are naturally a product of the sample orientation and the lack of correct core orientations for the majority of the samples means that the AMS data, similar to the remanence data, is of limited value.

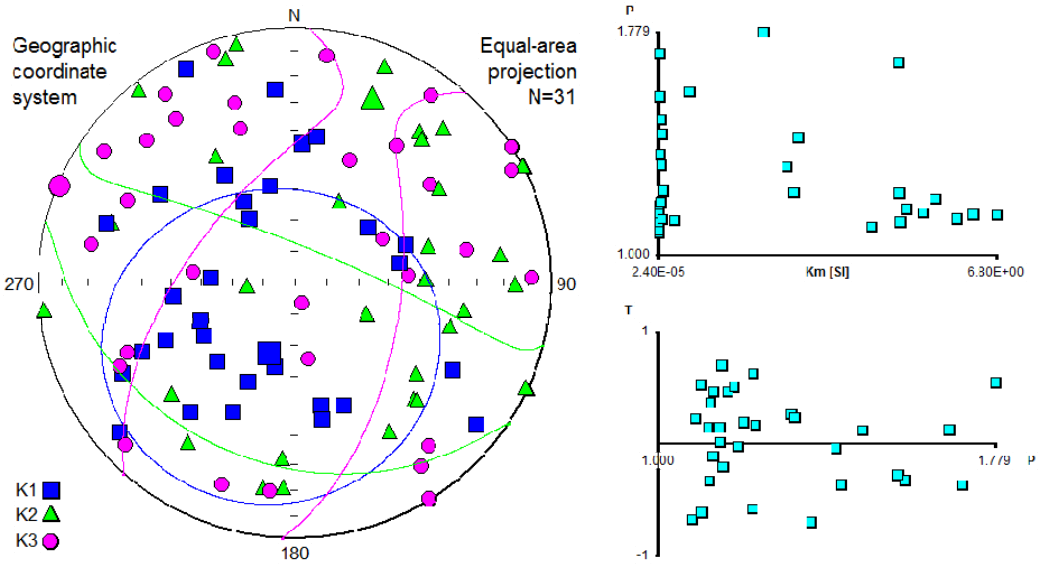

Figure 15: AMS results for all Osborne samples. P is the degree of anisotropy and T is a measure of the oblateness of the ellipsoid; positive = oblate (foliation), negative = prolate (lineation).

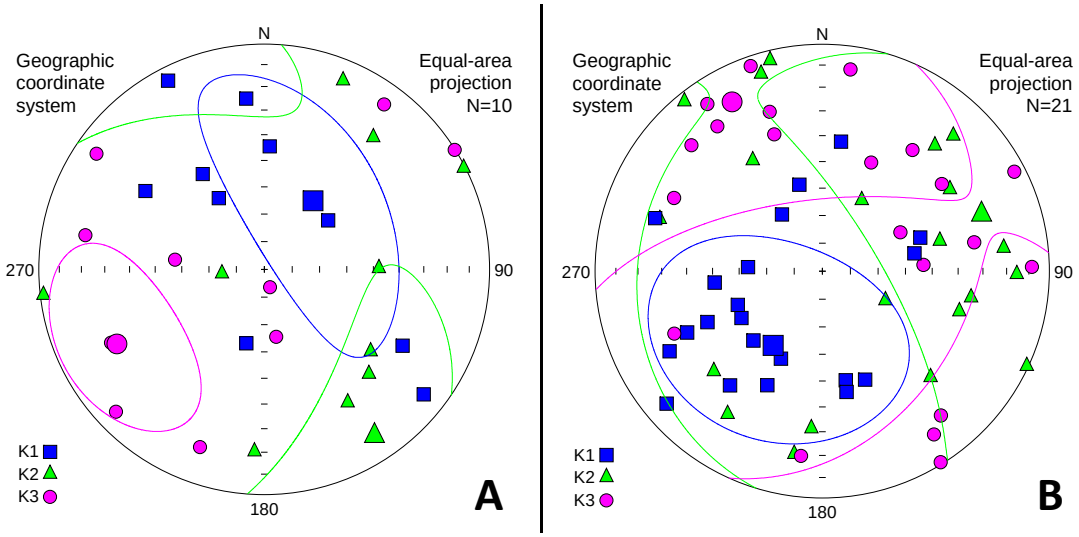

Figure 16: AMS results for samples from drill holes OSHQ0067 (A) and TTNQ0364 (B).

Once separated into the different drill holes, the results are clearer (Figure 16). It should be noted that despite the lack of orientation data, the results from both holes appear to cluster well. This may indicate that despite lack of orientation relative to geographic coordinates, the samples might be consistently oriented down individual holes or sections of hole.

Despite the small number of samples, the data from OSHQ0067 (Figure 16A) shows a trend of K1 and K2 vectors which form a NW-SE girdle dipping approximately 60° to the NE – indicating a SW-NE shortening. The AMS fabric appears to be coincident with local structures, in particular ENE – oriented zones of decreased magnetisation that appear to truncate the NNW-oriented magnetised zone at Osborne (Fig 17).

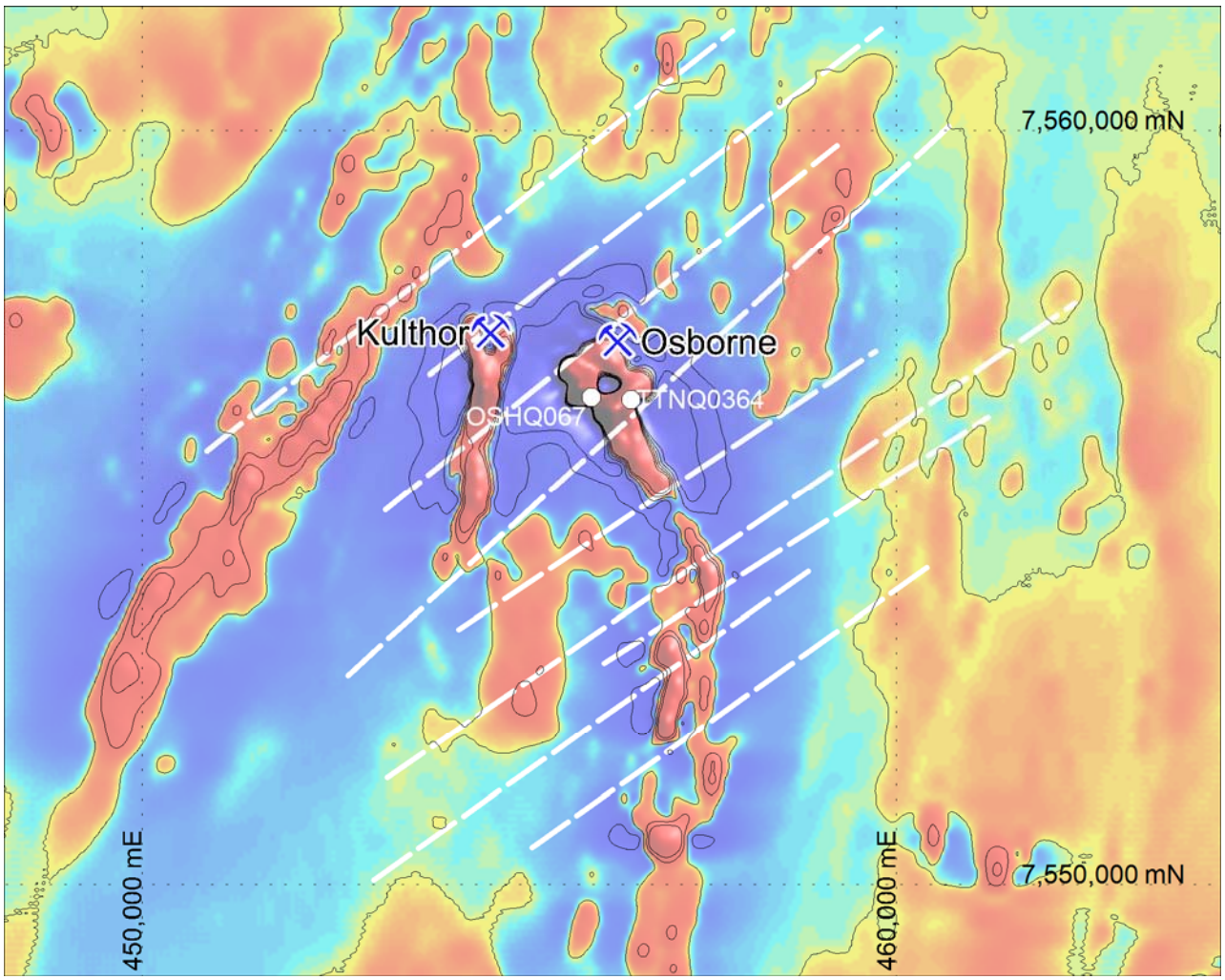

Figure 17: 1st vertical derivative of the reduced to pole magnetic data over the Osborne-Kulthor area, indicates that the main north to north-northwest magnetic high is truncated by a number of northeast to east-northeast structures.

This AMS fabric could be interpreted in a number of ways, including: 1. NE-SW shortening during D_3 caused a ENE- shearzone to form obliquely to the shortening direction, in which sinistral transpression occurred; 2. NW-SE shortening during D_4 caused mostly reverse shearing in a newly formed shearzone, which was oriented normal to the shortening direction. The AMS data inconjunction with our interpretation of the TIMA data suggest that the former is the more likely. Hence, we interpret that the AMS fabric formed during D_3 in conjunction with the biotite-mylonite style mineralisation.

7 Geophysics of the Deposit

Magnetic modelling of the Osborne deposit was not carried out as part of this study. Readers are referred to work completed by Clark (1988), Gidley (1988), Anderson and Logan (1992), and Ellis et al. (2012) who examine in-depth the various geophysical responses of the Osborne ore body. As stated in section 2.3, the Osborne deposit produces a large positive magnetic anomaly that is broadly coincident with EM and IP anomalies. The high magnetite content results in strong self-demagnetisation effects at Osborne which need to be properly accounted for when undertaking modelling of the magnetic response over the deposit (Clark, 1988).

8 Conclusion

The Osborne deposit is distinguished by paragenetically early magnetite, which is interpreted to represent a banded ironstone that formed during deposition of cover sequence 3, at the stratigraphic transition between the Mt Norna Quartzite and the Toole Creek Volcanics. The timing, at ca 1650 Ma, is temporally coincident with similar “BIFs” at a number of other deposits/prospects throughout the Eastern Succession (e.g., Monakoff, E1, Weatherly Creek, Maronan). Mineralisation at Osborne is, however, carried in rocks which do not fully preserve BIF-like fabrics. In many instances TIMA analyses indicate that chalcopyrite-rich samples preserve equigranular, metamorphic, fabrics which indicate that the deposit was affected by migmatisation, most likely during peak metamorphic conditions syn- to post-D2 (ca 1590 Ma). Several specimens also contain chalcopyrite in conjunction with retrograde- biotite assemblages, which formed during D3 (ca 1550 Ma), and are likely related to similar biotite mylonites in the Eastern Succession (e.g., the Cloncurry Fault Zone).

The magnetic susceptibility of the mineralised zone at Osborne is the highest recorded in the Uncover Cloncurry, with many values in the order of 2 SI. As such it is not surprising that it is coincident with such a high intensity magnetic anomaly. The remanence recorded in these specimen is typically sub-ordinate to Magnetic Susceptibility, with Q ratios of <1. However, the NRM values are likely inflated by approx. 300%, so the corrected Q’s are likely to be <0.3. Rocks with such coarse grained magnetite, typically do not preserve remanence in any case, due to the multidomain structure of the contained magnetite, so any remanent magnetisation present will likely be oriented parallel to the Earth’s magnetic field.

AMS data from the oriented hole (TTNQ0364) indicated a NE-oriented AMS fabric, with a shallow WSW-dipping K1 (lineation), and sub-horizontal, NNW-oriented K3. The fabric appears to be coincident with zones of decreased magnetisation that cut ENE-across the NNW-oriented magnetised zone at Osborne. This AMS fabric is interpreted to refect NE-SW shortening during D3 which caused a ENE- shearzone to form obliquely to the shortening direction, in which sinistral transpression occurred. This interpretation, inconjunction with evidence from the TIMA data suggests that the AMS fabric formed during D3 in conjunction with the biotite-mylonite style mineralisation.

9 References

Adshead, N.D., 1995. Geology, alteration and geochemistry of the Osborne Cu-Au deposit, Cloncurry District, N.W. Queensland, Australia. Ph.D. thesis, James Cook University, Townsville, Australia.

Adshead, N.D., Voulgaris, P., Muscio, V.N., 1998. Osborne copper–gold deposit. In: Berkman DA, Mackenzie DH Geology of Australian and Papua New Guinean mineral deposits. The Australasian Institute of Mining and Metallurgy, Melbourne, pp. 793–800.

Austin, J.R., Gazley, M.F., Walshe, J.L., Godel, B., leGras, M., and Patterson, B.O., 2016. Uncover Cloncurry – The Monakoff Cu-Au-U deposit: Integrated Petrophysical and Geochemical analyses. CSIRO, Australia, EP165042, pp. 50.

Clark, D.A., 1988. Magnetic Properties and Magnetic Signatures of the Trough Tank and Starra Copper-Gold Deposits. Eastern Mourn Isa Block. A report for the AMIRA project 78/P96B (Applications of Rock Magnetism). CSIRO Division of Exploration Geoscience, Australia.

Davidson, G.J., 1989. Starra and Trough Tank: Iron formation-hosted gold-copper deposits of northwest Queensland, Australia. Ph.D. thesis, University of Tasmania, Australia.

Davidson, G.J., 1992. Hydrothermal geochemistry and ore genesis of sea-floor volcanogenic copper-bearing oxide ores. Economic Geology, 87(3), pp.889-912.

Fisher, L., 2007. Hydrothermal processes at the Osborne Fe-Oxide-Cu-Au deposit, NW Queensland: integration of multiple micro-analytical data sets to trace ore fluid. Ph.D. thesis, James Cook University, Townsville, Australia.

Fisher, L.A. and Kendrick, M.A., 2008. Metamorphic fluid origins in the Osborne Fe oxide–Cu–Au deposit, Australia: evidence from noble gases and halogens. *Mineralium Deposita*, **43**, 483–497.

Gauthier, L., Hall, G., Stein, H., Schaltegger, U., 2001. The Osborne deposit, Cloncurry district: a 1595 ma cu-au skarn deposit. In: Williams PJ (ed) A hydrothermal odyssey extended conference abstracts, Townsville, 17–19 May, 58–59.

Gazley, M.F., Patterson, B.O., Austin, J.R., and Godel, B., 2016. Uncover Cloncurry – Summary of methods: Integrated Petrophysical and Geochemical analyses. CSIRO, Australia, EP166336, pp. 3.

Gazley, M.F., and Collins, K.S., 2016. Multivariate analyses of geochemical data from Cloncurry deposits. CSIRO, Australia, EP164972, pp. 24.

Gidley, P.R., 1988. The Geophysics of the Trough Tank Gold-Copper Prospect, Australia. Exploration Geophysics 19, 76–78.

Giles, D., Nutman, A.P., 2002. SHRIMP U-Pb monazite dating of 1600– 1580 Ma amphibolite facies metamorphism in the southeastern Mt Isa Block, Australia. Australian Journal of Earth Sciences 49, 455–466.

Giles, D. and Nutman, A.P., 2003. SHRIMP U–Pb zircon dating of the host rocks of the Cannington Ag–Pb–Zn deposit, southeastern Mt Isa Block, Australia. Australian Journal of Earth Sciences 50, 29–309.

Patterson BO, leGras M, Gazley MF, Austin JR, Godel B, Walshe JL, Hawkins S, Sisson M, Birchall R (2016): Uncover Cloncurry Data Pack. v1. CSIRO. Data Collection. http://doi.org/10.4225/08/5806a55f5797f

Perkins, C., and Wyborn, L.A.I., 1998. Age of Cu-Au mineralisation, Cloncurry district, eastern Mt Isa Inlier, Queensland, as determined by Ar-40/Ar-39 dating. Australian Journal of Earth Sciences 45, 233–246.

Rubenach, M.J., Adshead, N.D., Oliver, N.H.S., Tullemans, F., Esser, D., and Stein, H., 2001. The Osborne Cu-Au deposit: geochronology, and genesis of mineralization in relation to host albitites and ironstones. In: Williams PJ (ed) A hydrothermal odyssey, new developments in metalliferous hydrothermal systems research. EGRU Contribution 59, 172–173.

Rubenach, M.J., Foster, D.R.W., Evins, P.M., Blake, K.L. and Fanning, C.M., 2008. Age constraints on the tectonothermal evolution of the Selwyn Zone, Eastern fold belt, Mount Isa Inlier. Precambrian Research 163, 81–107.

Whitney D.L., and Evans, B.W., 2010. Abbreviations for names of rock-forming minerals. American Mineralogist 95, 185–187.

CONTACT US

t 1300 363 400
+61 3 9545 2176
e enquiries@csiro.au
w www.csiro.au

AT CSIRO WE SHAPE THE FUTURE

We do this by using science to solve real issues. Our research makes a difference to industry, people and the planet.

As Australia's national science agency we've been pushing the edge of what's possible for over 85 years. Today we have more than 5,000 talented people working out of 50-plus centres in Australia and internationally. Our people work closely with industry and communities to leave a lasting legacy. Collectively, our innovation and excellence places us in the top ten applied research agencies in the world.

WE ASK, WE SEEK AND WE SOLVE

FOR FURTHER INFORMATION

Mineral Resources / Geophysics
Jim Austin
t +61 2 9490 8876
e james.austin@csiro.au
w https://confluence.csiro.au/display/cmfr/Home

Mineral Resources / Geochemistry
Michael Gazley
t +61 8 6436 8501
e michael.gazley@csiro.au
w www.csiro.au/

Mineral Resources / Mineral Systems
John Walshe
t +61 8 6436 8643
e john.walshe@csiro.au
w www.csiro.au/